1 Introduction

In 2023, metal cutting machine tools valued at a total of € 8 billion were produced in Germany, accounting for 75 % of the total machine tool production volume. Flexible machining centers and milling machines made up 41 % of this share [VDW24]. The production of precision tools generated a turnover of € 10 billion in Germany in 2023 [ZEDW24]. Due to its high flexibility and wide range of applications, the milling process remains a key technology in modern manufacturing. For machining demanding materials such as hardened steels, nickel-based superalloys, and titanium alloys, the use of cutting fluid is essential for enhancing tool life, productivity, and process reliability by providing cooling, lubrication, and chip evacuation.

In aerospace applications, titanium alloys are especially common due to their favorable material characteristics, currently making up around 14 - 15 % of the total material mix in commercial aircraft [TAEN16]. The rising demand for air transport is expected to drive a 90 % increase in the demand for cutting tools used in titanium machining for aerospace between 2023 and 2026 [BERA23].

Reducing both economic and ecological costs in production is crucial for maintaining competitiveness, particularly in high-wage countries such as Germany. The primary cost drivers in milling titanium structural components include labor, as well as tool and cutting fluid costs, suggesting significant potential for cost reduction through process improvements [LANG19]. Key factors for creating a more economical and environmentally friendly process include reducing the consumption of cutting tools, cutting fluid, and electrical energy in both the machine tool and its peripheral units [DENK20].

Innovative tool concepts, such as those with optimized internal cutting fluid supply, have demonstrated improved tool life, productivity, and process reliability in drilling, turning, and milling [CAYL17; LAKN21a; OEZK17; SANG13]. However, conventional manufacturing of cutting tools with complex internal channel structures is both costly and limited in geometric complexity. The design flexibility offered by additive manufacturing (AM) processes, such as Laser Powder Bed Fusion (PBF-LB), presents significant potential for developing customized, individualized, process-adapted, and efficient cutting fluid supply systems.

However, there is a lack of fundamental understanding regarding the cause-effect relationships between the AM process, cutting fluid supply characteristics, and tool performance during machining. This work aims to gain better knowledge and design guidelines for the internal cutting fluid supply in AM milling tools, tailored to specific process boundary conditions. The geometric characteristics for a focused and low-loss cutting fluid supply are systematically varied in indexable AM milling tools, and the dependency of cutting fluid supply characteristics and engagement conditions on tool load and machinability is analyzed. The improved machining performance of the AM tools is evaluated and validated both economically and ecologically. Thus, this work builds the foundation for designing and applying AM milling tools with an adapted cutting fluid supply.

Einleitung

Im Jahr 2023 wurden in Deutschland spanende Werkzeugmaschinen mit einem Gesamtwert von 8 Mrd. € hergestellt. Flexible Bearbeitungszentren und Fräsmaschinen hatten daran einen Anteil von 41 % [VDW24]. Präzisionswerkzeuge erwirtschafteten in Deutschland im Jahr 2023 einen Umsatz von 10 Mrd. € [ZEDW24]. Das Fräsen stellt aufgrund der hohen Flexibilität und des breiten Anwendungsspektrums nach wie vor eine Schlüsseltechnologie in der modernen Fertigungstechnik dar. Bei der spanenden Bearbeitung anspruchsvoller Werkstoffe wie gehärteten Stählen, Nickelbasis- oder Titanlegierungen ist der Einsatz von Kühlschmierstoffen (KSS) essenziell, um die Werkzeuglebensdauer, die Produktivität und die Prozesssicherheit zu erhöhen.

In der Luft- und Raumfahrt sind Titanlegierungen aufgrund ihrer vorteilhaften Materialeigenschaften besonders verbreitet und machen derzeit etwa 14 bis 15 % des Materialmixes in Verkehrsflugzeugen aus [TAEN16]. Aufgrund der steigenden Nachfrage nach Luftverkehrsmitteln wird zwischen 2023 und 2026 mit einer Nachfragesteigerung von 90 % für Zerspanwerkzeuge zur Titanbearbeitung gerechnet [BERA23]. Die Senkung der ökonomischen und ökologischen Kosten in der Produktion ist entscheidend für den Erhalt der Wettbewerbsfähigkeit, insbesondere im Hochlohnland Deutschland. Da die Hauptkostentreiber beim Fräsen von Titanbauteilen neben den Lohnkosten insbesondere in den Werkzeug- und KSS-Kosten liegen, ist hier ein erhebliches Potenzial zur Kostensenkung durch Prozessverbesserungen vorhanden [LANG19].

Durch ein Einsatz einer internen KSS-Zufuhr konnten beim Bohren, Drehen und Fräsen erhebliche Steigerungen von Standzeit, Produktivität und Prozesssicherheit erzielt werden [CAYL17; LAKN21a; OEZK17; SANG13]. Die konventionelle Fertigung von Zerspanwerkzeugen mit komplexen inneren Kanalstrukturen ist jedoch kostenintensiv und in der abbildbaren geometrischen Komplexität begrenzt. Aufgrund der gesteigerten geometrischen Gestaltungsfreiheit ist durch additive Fertigungsverfahren wie dem Laser Powder Bed Fusion (PBF-LB) die Entwicklung und Fertigung individueller, prozessangepasster und verlustarmer KSS-Zufuhrkonzepte möglich.

Bisher fehlt es in der Fräsbearbeitung allerdings an grundlegendem Verständnis der Ursache-Wirkungs-Zusammenhänge zwischen der additiven Fertigung, der KSS-Zufuhrcharakteristik, und dem Einsatzverhalten des Werkzeugs. Ziel dieser Arbeit ist daher die Untersuchung der Potenziale einer internen, prozesspezifisch angepassten KSS-Zufuhr im Fräsen sowie die Ableitung von Richtlinien zur Auslegung ebendieser. Die geometrischen Merkmale für eine fokussierte und verlustarme KSS-Zufuhr werden in plattenbestückten, additiv gefertigten Messerkopffräsern systematisch variiert und der Einfluss von KSS-Zufuhrcharakteristik und Eingriffsbedingungen auf Werkzeugbelastung und Einsatzverhalten analysiert. Die verbesserte Werkzeugperformance der additiv gefertigten Werkzeuge wird sowohl ökonomisch als auch ökologisch bewertet und validiert. Damit bildet die vorliegende Arbeit die Grundlage für die Auslegung und den Einsatz additiv gefertigter Fräswerkzeuge mit angepasster KSS-Zufuhr.

2 State of the art

Stand der Technik

This chapter presents the fundamentals relevant to this work and provides an overview of the current state of knowledge in the fields of milling, cutting fluid supply, and additive manufacturing. First, the focus is placed on the milling process, with particular emphasis on its kinematics, the resulting thermo-mechanical loads, and the associated tool wear phenomena. Next, the modes of action of cutting fluids in machining are explored, focusing on the thermal, mechanical, and lubricating mechanisms and the influence of cutting fluid supply parameters on the machining process. Finally, the principle of additive manufacturing, specifically PBF-LB, is introduced as the relevant process for this work. The potential applications of this manufacturing technique in the context of cutting tools are also identified. Based on this review, the knowledge and research gaps addressed in this work are derived.

Parts of this chapter have been published in Metals (2024), Volume 14, Issue 9 [KELL24a].

2.1 Thermo-mechanical tool load in milling

Thermomechanische Werkzeugbelastung im Fräsen

The thermo-mechanical load in the cutting process is determined by a combination of workpiece-dependent, tool-dependent, and process-specific influencing variables. These variables are often interdependent and complex to isolate [WALT98, p. 9]. The characteristics of the milling process, such as the interrupted cut, varying chip thickness, and rotational tool movement, introduce additional complexities compared to continuous cutting processes like turning. The following chapter addresses the milling process and its thermal aspects, focusing on identifying the predominant tool wear phenomena.

2.1.1 Kinematics and heat generation

Kinematik und Wärmeentwicklung

The thermo-mechanical load on the tool during milling is influenced mainly by the geometrical engagement conditions, particularly the process kinematics. As the tool tooth follows a trochoidal path, the engagement forms a non-uniform area described by the undeformed chip thickness h. Figure 2.1 illustrates the engagement conditions in peripheral down milling. In the first phase of chip formation (I, $\Phi_{en} \leq \Phi \leq \Phi_{max}$), the tool with diameter D engages the workpiece until the maximum undeformed chip thickness, h_{max}, is reached. The undeformed chip thickness decreases to zero at the end of the second phase (II, $\Phi_{max} \leq \Phi \leq \Phi_{ex}$), when the tool tip exits the workpiece [MART41]. The tool entry with h = 0 mm in up milling causes friction between the flank face and the workpiece and can promote tool wear. For this reason, down milling is generally preferred, especially for difficult-to-cut materials [KLOC18a, p. 358]. Neglecting the cycloidal nature of the tool tip movement and assuming a circular motion is permissible

when the cutting speed v_c is much greater than the feed velocity v_f ($v_c >> v_f$) [KRON69]. Under this assumption, the effective, mean, and maximum undeformed chip thicknesses h, h_m and h_{max} as well as the length of cut l_c can be expressed as [KRON69; MART41]:

$$h(\Phi) \approx h_{II}(\Phi) = \frac{D}{2} + f_z \cdot sin(\Phi) - \sqrt{\frac{D^2}{4} - (f_z \cdot cos(\Phi))^2} \approx f_z \cdot sin(\Phi) \quad 2.1$$

$$h_{max} = f_z \cdot sin(\Phi_{en}) \quad 2.2$$

$$h_m = \frac{1}{\Phi_c} \cdot f_z \cdot (cos\,(\Phi_{en}) - cos\,(\Phi_{ex})) = \frac{1}{\Phi_c} \cdot f_z \cdot \left(2 \cdot \frac{a_e}{D}\right) \quad 2.3$$

The undeformed chip thickness directly affects the local mechanical load on the cutting edge. The influence of various parameters, such as tool diameter D, width of cut a_e, and feed per tooth f_z, on the undeformed chip thickness h is shown in Figure 2.1. The radial immersion a_e/D significantly impacts the contact angle Φ_c and, consequently, the angle- and time-dependent undeformed chip thickness h. The maximum undeformed chip thickness h_{max} increases with greater radial immersion, which can result from either increasing the width of cut or decreasing the tool diameter. Simultaneously, these cutting parameters affect the length of cut l_c, as well as the engagement respective heating and cooling periods during each tool rotation.

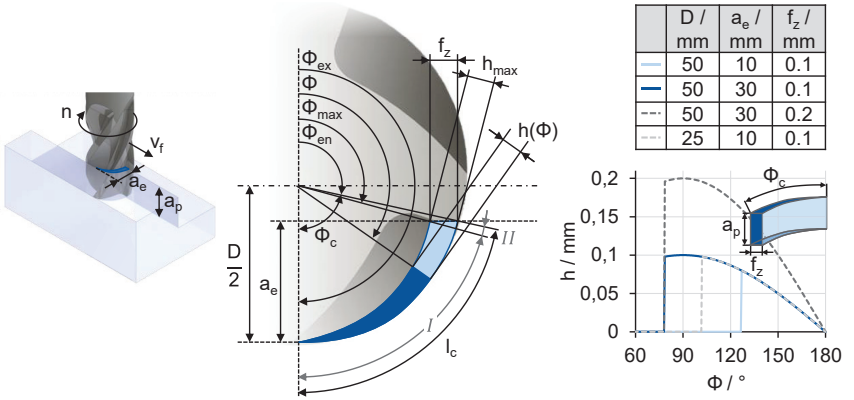

a_e : Width of cut	h(Φ) : Undeformed chip thickness	Φ : Cutter rotation angle
a_p : Depth of cut	h_{max} : Max. undeformed chip thickness	Φ_c : Contact angle
f_z : Feed per tooth	n : Rotational speed	Φ_{en} : Cutter entry angle
l_c : Length of cut	v_f : Feed velocity	Φ_{ex} : Cutter exit angle

Figure 2.1: Kinematics of the peripheral down milling process and cutter rotation angle dependent undeformed chip thickness for different cutting parameters (based on [AUGS18, p. 5; MEIN09, p. 69])
Kinematik des Umfangsfräsprozesses und Werkzeugdrehwinkel in Abhängigkeit der Spanungsdicke für verschiedene Schnittparameter

The engagement period during a single tool rotation, composed of cutting time t_c and non-cutting time t_{nc}, is illustrated in Figure 2.2 (a) for different radial immersions. Contact angle, cutting time and non-cutting time do not vary linearly with changes in width of cut and radial immersion. The maximum ratio between cutting time and non-cutting time (1:1) is reached in full-slot milling. As shown by KRONENBERG, the engagement time is slightly shorter in down compared to up milling, though this effect is minimal compared to the influence of width of cut on engagement time [KRON69, p. 27].

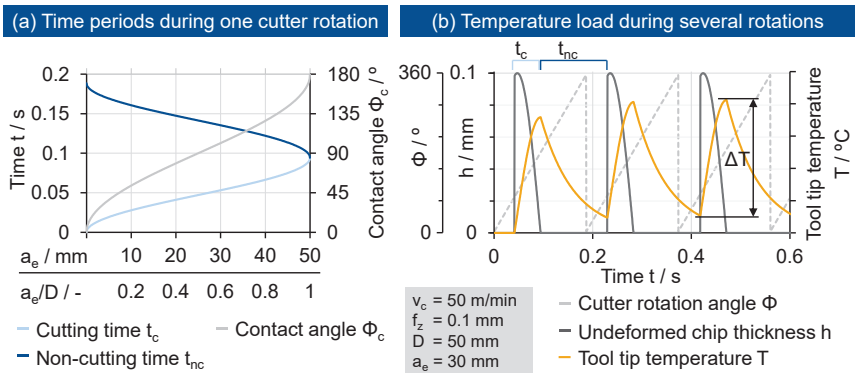

Figure 2.2: Cutting time and non-cutting time in peripheral down milling for different radial immersions and resulting temperature load at the tool tip for several rotation cycles (exemplary calculation based on [PÁLM87; SATO11])
Schnitt- und Nebenzeit im Umfangsfräsen für unterschiedliche radiale Eingriffsverhältnisse sowie resultierende Temperaturbelastung auf der Schneidkante für mehrere Werkzeugumdrehungen

The alternating cutting force due to the varying chip formation can be approximated with the empirical KIENZLE equation, considering the width of undeformed chip b (equals depth of cut a_p for cutting edge angle κ_r = 90°) and the material-specific constants $k_{c1.1}$ and m_c [KIEN52; KLOC18a, p. 541]:

$$F_c = b \cdot k_{c1.1} \cdot h(\Phi)^{1-m_c} \qquad 2.4$$

The corresponding cutting power P arising during the process as the product of cutting and feed velocity and the equivalent cutting force components can be described as:

$$P = P_c + P_f = v_c \cdot F_c + v_f \cdot F_f \approx v_c \cdot F_c \quad (\text{for } v_c \gg v_f) \qquad 2.5$$

The cutting power is mainly transformed into heat due to cutting, shearing, and friction between the tool and the workpiece [KLOC18a, p. 73].

The cyclical, recurring mechanical and resulting thermal load of the milling process is displayed in Figure 2.2 (b) for several engagement cycles. During the engagement period, the generated heat Q causes a sharp increase in temperature ΔT in the tool through the heat input in the tool-chip contact area. As the contact area and cutting power P depend on the undeformed chip thickness, the heat source surface and heat amount constantly change over time [SATO11]. During the non-cutting time interval

t_{nc}, the tool tip cools down due to heat conduction into the cutting wedge. The low heat conductivity of most tool substrate materials (tungsten carbide: 116 W/mK vs. aluminum: 236 W/mK) delays the heat penetration into the interior of the tool [OPIT63, p. 36]. WANG ET AL. observed a negligible amount of forced convection into the surrounding air in dry milling, concluding that the maximum temperature arises on the rake surface in the tool-chip contact area [WANG96]. Thus, the temperature in the tool-chip interface strongly depends on the thermal diffusivity of the workpiece material and tool substrate [LIN95]. The heat flow $\dot{Q}$ into the tool depends not only on the absolute temperature in the contact area, but also on the temperature difference between surface and interior volume of the tool. Therefore, the amount of heat flow into the tool changes as a function of the number of milling cycles.

Due to the heating of the cutting wedge, the maximum tool tip temperature is only reached after several engagement cycles [PÁLM87]. Heat flux and temperature did not reach a stable level after 100 milling cycles in dry milling of AISI 4140 based on the numerical model presented by NEMETZ ET AL. [NEME19]. Contrary, WU ET AL. observed stable peak temperatures after 10 cycles in interrupted cutting of AISI 1045 according to numerical calculations [WU79]. AUGSPURGER observed progressively increasing temperature fluctuations in distances below 0.5 mm to the tool tip and nearly constant temperature in greater distance [AUGS18, p. 118]. UEDA ET AL. found temperatures on the flank face to be slightly higher in the tool corner and at the depth of cut [UEDA01].

JIAN ET AL. demonstrated that the ratio between cutting and non-cutting time affects the rise in tool temperature for a constant cutting speed and heat flow into the tool [JIAN13]. Longer cutting times lead to higher tool temperatures due to increased heat generated during engagement. Furthermore, increased length of cut l_c resulting from a higher radial immersion provokes a deeper heat penetration into the cutting wedge due to the increased contact time between tool and workpiece. Short cutting times lead to nearly constant tool temperatures. As stated by AUGSPURGER, the heat flow into the tool increases with increased cutting speed, leading to higher tool tip temperatures even though the absolute cutting time decreases [AUGS18, p. 94; PUTZ17]. OKUSHIMA ET AL. measured a linear increase in tool tip temperature with a logarithmic increment of either cutting speed or feed per tooth in milling of carbon steel with tungsten carbide tools [OKUS67].

Alongside with the cutting parameters, the workpiece material determines the load applied to the tool, expressed by the material constants in Eq. 2.4. In orthogonal cutting experiments with the same process parameters, AUGSPURGER ET AL. measured 25 % higher cutting forces for Inconel 718 compared to AISI 1045 (C45E) and 44 % higher forces compared to Ti-6Al-4V [AUGS19b]. Due to the differing material characteristics, the heat flow into the tool was higher for Inconel 718 compared to AISI 1045, leading to higher tool temperatures in peripheral milling [AUGS18, p. 114]. Thus, the workpiece material influences maximum temperature and temperature fluctuations.